Silver Nanoparticles-Based Substrate for Blood Serum Analysis under 785 nm Laser Excitation

Sahar Z. Al-Sammarraie[1*], Lyudmila A. Bratchenko[1], Elena N. Typikova[1], Peter A. Lebedev[2], Valery P. Zakharov[1], and Ivan A. Bratchenko[1]

[1] Samara University, 34 Moskovskoe shosse, Samara 443066, Russian Federation

[2] Samara State Medical University, 39 Chapaevskaya str., Samara 443099, Russian Federation

*** e-mail:** saharzead@rocketmail.com

Abstract. Individuals who have different diseases need a routine assessment of their body metabolism, and the methods that used are practically difficult, inconvenient or expensive. The objective of this study was to develop a technique of human blood serum analysis that is simple, reliable and fast, and based on a surface-enhanced Raman spectroscopy (SERS). In this study, serum samples were examined using conventional Raman (CR) and SERS. The observed CR and SERS bands were analyzed. Several of these bands (724, 813, 890, 961, and 1132 cm^{-1}) clearly stand out by the impact of the SERS technique, as the intensities of these bands in CR measurements are weaker than the intensity of the autofluorescence and noise. The Enhancement Factor (EF) was up to 4×10^5. Stability of the proposed SERS technique was confirmed by the measurements of signal standard deviation. The observed standard deviation does not exceed 19% for different SERS substrates and does not exceed 8% in case of a single SERS substrate measurements. The obtained results demonstrate that the proposed SERS technique is stable and has significant potential in clinical diagnosis applications.

Keywords: surface-enhanced Raman spectroscopy; Enhancement Factor; blood serum; silver nanoparticles; Raman band shift.

Paper #3461 received 1 Nov 2021; revised manuscript received 24 Jan 2022; accepted for publication 24 Jan 2022; published online 3 Feb 2022. doi: 10.18287/JBPE22.08.010301.

1 Introduction

The biggest threat to human life and health is a disease, according to death causes statistics provided by the World Health Organization [1]. Numerous diseases are caused by lifestyle behaviors, environmental pollution, occupational hazards, biological and natural factors, chronic intoxication and trauma, iatrogenic factors, and other external factors; and certain diseases are fatal [2, 3]. As a result, the most effective strategies to increase patient survival are early diagnosis and therapy [4]. That is why it is important for individuals who have different diseases to perform a routine assessment of their body functions. Health screening programs are central to the public health system. In order to analyze the functional and pathological processes of the human body, laboratory analyzes of body biofluids are widely used. Many studies on the human body and the investigation of disease processes are done at the level of single cells, proteins, and genes [5–7]. As a result, there is a growing demand for disease diagnostic and analysis technologies. It is necessary to establish a variety of measuring methods and standards for the early detection of various illnesses. Recently, biomarkers have been increasingly utilized in illness diagnosis to signal definite or possible changes in the structure or function of systems, organs, tissues, and cells. It should be noted that laboratory methods used today in clinical practice have a number of limitations.

Recently, Raman spectroscopy has been used to detect viruses, identify bacteria, analyze cells, and make clinical diagnoses [8–14]. Because of its multiple detection capabilities, single-molecule level sensitivity, and quantitative ability, Raman spectroscopy's unique spectral feature makes it an excellent label-free, reliable, and fast diagnostic tool since it can analyze chemical components such as proteins, nucleic acids [6–10], and carbohydrates in biological materials. Surface-enhanced Raman spectroscopy (SERS) has been extensively investigated for biological applications [2–5]. SERS is

recognized as an ultrasensitive optical detection technique with wide application potential in a variety of fields due to its great sensitivity at the single-molecule level.

However, the limitations of the SERS technique are (1) the method requires intimate contact between the enhancing surface and the analyte; (2) the substrates degrade with time resulting in a decrease in the signal; (3) limited selectivity of the substrates for a given analyte; (4) limited re-usability of the substrates; and (5) problems with homogeneity and reproducibility of the SERS signal within a substrate [15]. In this regard, novel approaches of SERS signal registration from the biological fluids are in a high demand. Optimization of methodology of SERS substrates preparation and SERS spectra acquisition requires new approaches to create fast, low-cost and reliable techniques of biofluids chemical sensing.

Thus, in the current study, a simple approach of SERS substrate implementation for blood serum analysis is considered. Blood serum or blood components is a biofluid that is widely used as a diagnostic sample since it is rich in biochemical and biological information, is easily accessible, and can be obtained noninvasively. For the same reasons, it is often saved in biobanks for research purposes. In general, it is a metabolite pool generated from almost all of the human body's organs and tissues. As a result, Raman spectroscopy of human blood samples can be used to monitor metabolic changes caused by illnesses [16–20]. Serum has regularly been investigated using the SERS approach. For instance, Bonifacio et al. [21] employed aqueous Au and Ag colloids in combination with three lasers ranging from visible to near-infrared to perform a systematic study of SERS spectra of blood serum and plasma. However, the SERS spectra analysis indicated that strong and reproducible spectra can be generated rapidly only if proteins are eliminated from samples and a near-infrared excitation is employed in combination with Ag colloids. While Cao et al. [22] investigated the spectral properties of human blood for the purpose of detecting lung adenocarcinoma, lung squamous carcinoma, and large cell lung cancer using SERS spectroscopy on a highly branched gold nanoparticle substrate. They showed that SERS spectroscopy was a sensitive analytical tool for cancer classification and discriminating. Scientific group of Pérez et al. [23] was the first to employ SERS spectroscopy to identify Chagas disease in blood serum using concentrated silver nanoparticles and chemometric techniques. They achieved great accuracy when classifying samples into three categories (healthy patients and asymptomatic patients). However, even when the appropriate experimental parameters are established, significant care must be given while planning research for the development of diagnostic tests. Blood serum, like other biological objects, contains a number of fluorophores and is characterized by the presence of fluorescence [24, 25]. It should be noted that fluorescence is background and noise for the Raman signal. In order to reduce the contribution of fluorescence to the signal in the study of biological objects, the excitation of spectra in the near infrared range is widely used. Therefore, excitation of the spectral characteristics is realized at a wavelength of 785 nm. It is advisable to use particles of silver, copper or gold to achieve surface enhancement of the Raman signal in the near infrared region [26–28]. Colloidal silver solution is characterized by simplicity of preparation.

In the current work to implement a simple analysis of human serum using SERS, a silver SERS substrate was prepared. The goal of this work was to develop a SERS technique based on sliver nanoparticles (Ag NPs) application for simple, reliable and rapid analysis of human serum. To assess the prospects of the proposed SERS technique, the stability of SERS substrates and a comparative analysis of the conventional Raman (CR) spectra and SERS characteristics of serum samples with the calculation of the enhancement factor (EF) were carried out.

2 Materials and methods

2.1 Colloidal silver nanoparticles solution

Silver nitrate and trisodium citrate were used as starting materials for the preparation of (AgNPs). The silver colloid was prepared by using chemical reduction method. All solutions of reacting materials were prepared in distilled water. In typical experiment 20 ml of distilled water heated to boil. To this solution 3 ml of 1.8% $AgNO_3$ of and 6 ml of 1% trisodium citrate ($Na_3C_6H_5O_7$) were added. The resulting solution was heated at 95 °C for 20 min until a yellow-green solution is formed. Then the solution was removed from the heating device and stirred until cooled to room temperature. The UV-Vis spectrum of the AgNPs solution was obtained by utilizing the Spectrophotometer (UNICO 1201, United Products & Instruments, USA). The obtained absorption spectrum of AgNPs solution is shown in Fig. 1 and demonstrates an absorption maximum at 410 nm with a full width at half-maximum of 40 nm, which corresponds to spherical nanoparticles with 20 nm in diameter.

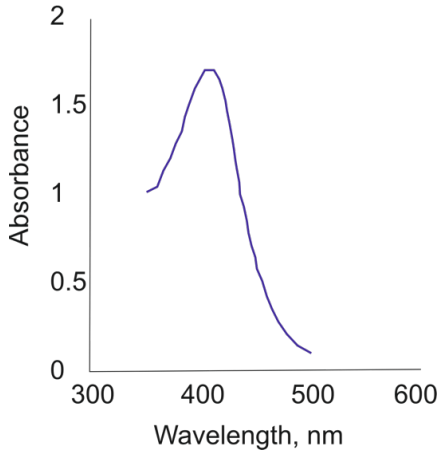

Fig. 1 UV-Vis absorbance spectrum of the colloidal AgNPs.

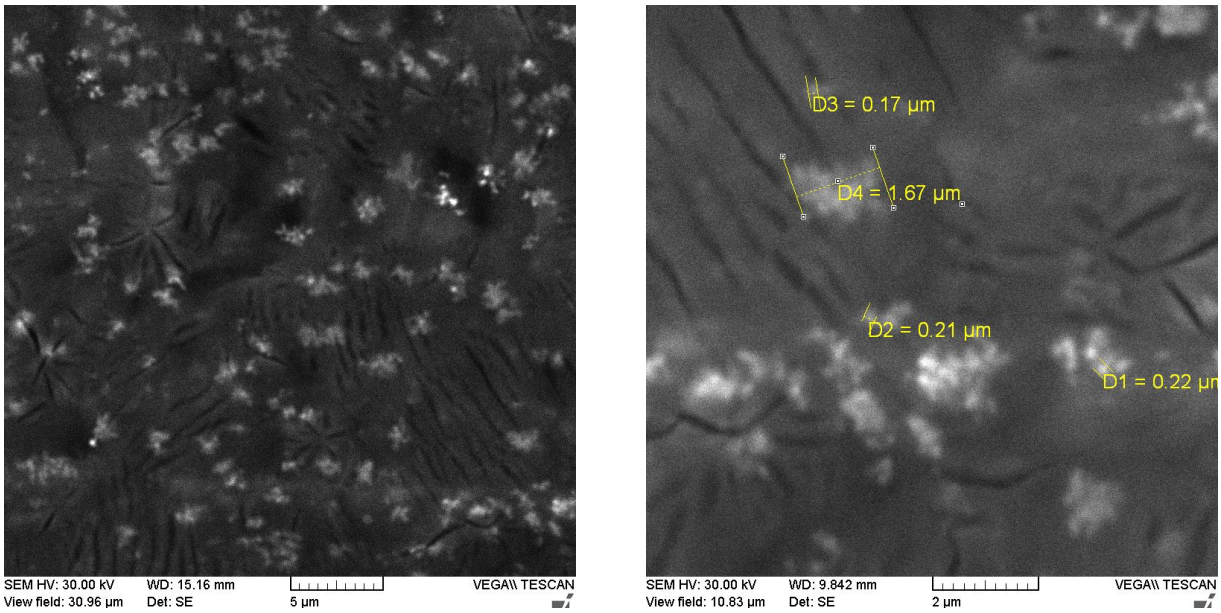

(a) (b)

Fig. 2 The electron-microscopic images of the substrate with silver particles at magnification factors of 7 000× and 20 000×.

The resulting colloidal solution with a volume of 20 ml was poured onto an aluminum foil with an area of 75 mm × 25 mm and dried at room temperature until completely dry. Fig. 2 presents the electron-microscopic images of the prepared substrate after drying. The electron-microscopic images of the substrate with silver structures were obtained on a Vega SB scanning electron microscope (Tescan, Czech Republic) with an INCA X-act energy dispersive X-ray analyzer (Oxford Instruments, the United Kingdom) at an accelerating voltage of 30 kV. The images contained agglomerates of spherical particles about 200 nm in size.

2.2 Serum samples preparation

A standardized sampling was carried out from patients of the Samara Regional Clinical Hospital named after V. D. Seredavin. The study included patients with stages 1–3a of chronic kidney disease. The study protocols were approved by the ethical committee of Samara State Medical University. All the subjects who participated in this study gave their written informed consent at the beginning of the study. The blood serum samples were collected from patients in fasting condition and placed in sealed containers, followed by freezing at a temperature of –16 °C. Immediately before the start of the analysis, the blood serum samples were defrosted at room temperature.

Each blood serum samples were dropped in a volume of 1.5 µl and dried for 30 min:

- on aluminum foil for CR analysis;
- on aluminum foil with the layer of dried silver colloid for SERS analysis.

2.3 Experimental setup and spectra collection

The experimental setup for Raman analysis of human serum includes a spectrometric system (EnSpectr R785, Spektr-M, Chernogolovka, Moscow Region, Russia) and a microscope (ADF U300, ADF, China). Focusing the exciting radiation and collecting the scattered radiation were implemented using 50× Objective LMPlan. The stimulation of collected spectra was performed by the laser module with central wavelength 785 nm. The diameter of the laser spot at the focus on the sample surface was 5 µm. The laser power was 10 mW for the SERS technique and 60 mW for the CR technique. Exposure time was 4 s for SERS and 20 s for CR. The resulting raw spectrum for each sample is an automatic sequential recording of four spectra with subsequent averaging. Thus, the recording time of the CR raw spectrum is 80 s, and 16 s for SERS.

The analyzed serum sample was examined 15 times in the same position and condition and then examined for 5 different SERS substrates at 5 different spots to indicate the accuracy and stability of the proposed SERS substrates in comparison to CR.

2.4 Spectra processing and calculation of enhancement factor (EF)

The analysis of the stability of the SERS substrate and the reproducibility of the result was carried out on raw spectra without preprocessing. The raw spectral data were subjected to calculating the mean spectrum and standard deviation. Calculation of standard deviation was performed in a standard manner [15]. The mean CR spectra and SERS spectra and shift peaks were assigned to the molecular structures and biochemical components based on the analysis of available studies.

The estimation of the EF is realized in a comparative analysis of the preprocessed CR and SERS spectra. Raw spectra were processed by carrying baseline correction and smoothing to remove noise and fluorescence background. Prior to analysis, the raw spectral data were smoothed by the Savitzky-Golay filter. Savitzky-Golay

filter was applied with filter window width of 15, 1 order of polynomial used for smoothing and 0 order of derivative to take (no derivative). Smoothing aims to remove noise and outliers from a given set of experimental data. Proper smoothing will act to increase the signal-to-noise ratio and enhance the primary features embedded in a given data-set. Numerical means whereby Raman spectral data may be smoothed have been widely employed in the field for many years [18, 29]. Baseline correction is based on polynomial approximation method (tenth-order polynomial function) to separate the autofluorescence and the Raman signal [28]. After spectral processing EF is estimated by the following equation:

$$EF = \frac{I_{SERS} \times EV_{Raman} \times C_{Raman} \times P_{Raman}}{I_{Raman} \times EV_{SERS} \times C_{SERS} \times P_{SERS}}, \quad (1)$$

where I_{SERS} and I_{Raman} are the intensities of the same band for the SERS and CR spectra, respectively; EV_{SERS} and EV_{Raman} are the exposure times for the SERS and CR spectra, respectively; C_{SERS} *and* C_{Raman} are the sample concentration for the SERS and CR spectra, respectively; P_{SERS} and P_{Raman} are the exciting laser power for the SERS and CR spectra, respectively. Since the CR and SERS spectra of the same sample were recorded to calculate the EF, the concentration ratio C_{Raman} / C_{SERS} is equal to 1 ($C_{Raman} = C_{SERS}$).

3 Results and discussion

At the first stage, the characteristic spectral features of a human serum sample using the SERS technology, using the CR technology, and the spectral characteristics of the prepared silver SERS substrate were considered. Fig. 3 shows the recorded raw SERS and CR spectra of serum. Fig. 4 demonstrates the preprocessed SERS and CR spectra of human serum corresponding to the Raman contribution. As can be seen from Fig. 3, the spectral contribution of the silver substrate to the SERS spectrum of the serum sample is insignificant. Consequently, when analyzing the SERS spectrum of serum obtained using the proposed approach, the spectral features characterize the tested serum sample and there is no need to take into account in the analysis the foreign contribution of the substrate. Only a few Raman peaks could be observed in the regular Raman spectra of the serum sample. The SERS spectra of the serum sample, obtained with the proposed technique with AgNPs shows multiple distinctive peaks, and the intensity of these peaks is enhanced compared with that of CR spectra.

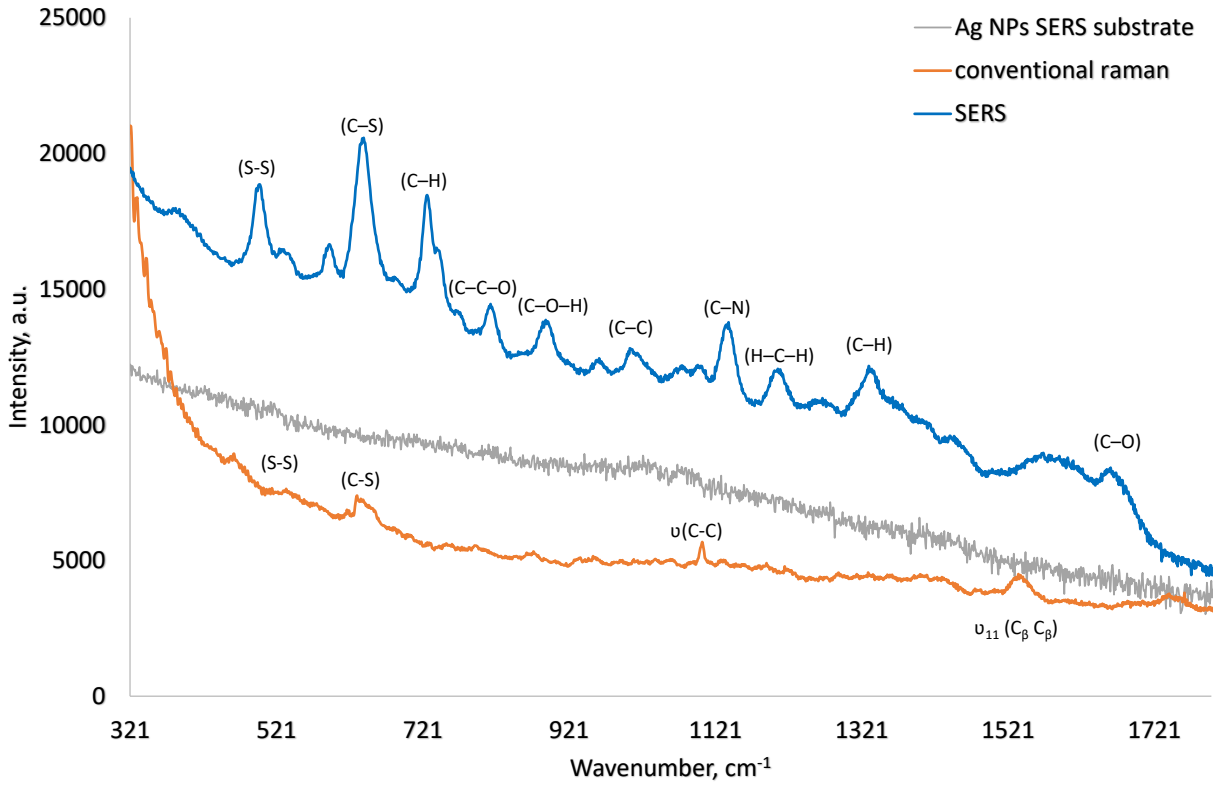

Fig. 3 Comparison of the raw spectrum of a blood serum sample for CR, SERS, and the spectral characteristics of the silver substrate.

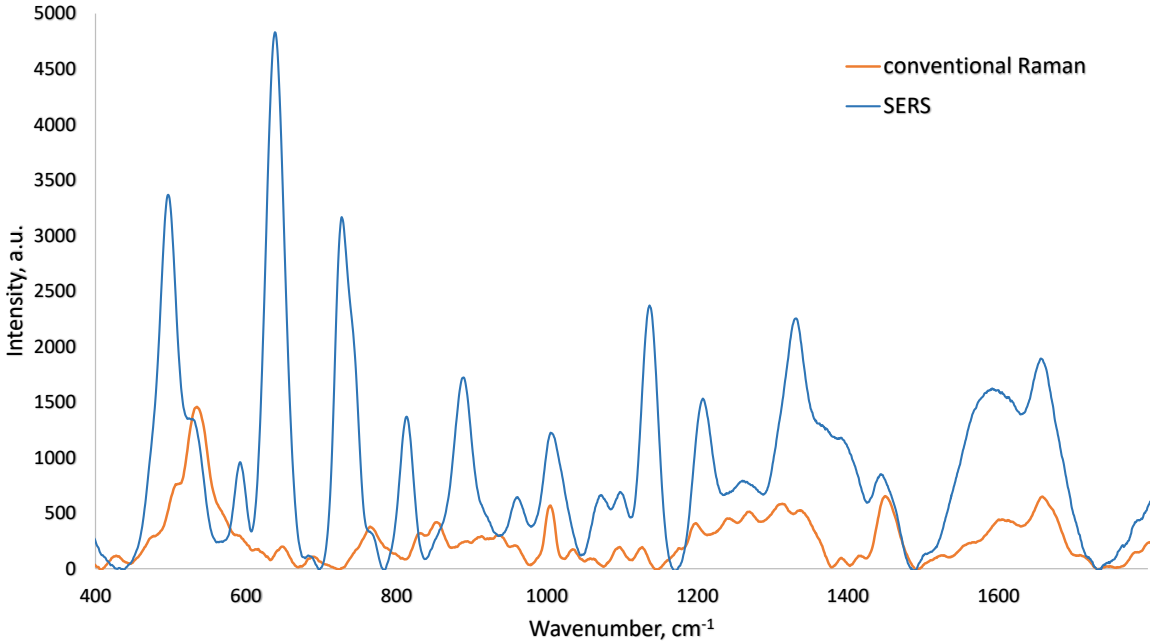

Fig. 4 Comparison of the preprocessed CR and SERS spectra of the same blood serum sample.

Table 1 Peak positions and their characteristic assignments.

Raman shift (cm^{-1})	**Peak assignment**	**Ref.**
Conventional Raman		
525	(S-S) disulfide stretching in proteins Phosphatidylserine	[37, 38]
641	(C–S) L-tyrosine, lactose	[39]
770	(C–H) Hypoxanthine, Phosphatidylserine	[40–43]
1100	υ(C-C)-lipids, fatty acids	[44]
1543	$\upsilon_{11}(C_\beta\ C_\beta)$, tryptophan	[45–46]
1661	(C–O) Amide I, α-helix	[40–43]
SERS		
498	(S-S) disulfide stretching in proteins Phosphatidylserine	[37, 38]
641	(C–S) L- tyrosine, lactose	[39]
728	(C–H) Hypoxanthine, Phosphatidylserine	[37, 38]
813	(C–C–O) L-Serine, glutathione	[37, 38]
890	(C–O–H) Glutathione, D-(C)-galactosamine	[37, 38]
961	υ (C-C), Cholesterol	[37, 38]
1003	(C–C) Phenylalanine	[39]
1086	(C-N) Stretching, Phosphodiester groups in nucleic acids	[37, 38]
1094	(C–N) Stretching mode in D-mannose	[47]
1132	(C-N) Ascorbic acid, L-serine	[37, 38]
1210	$C\text{-}C_6H_5$ stretching, L-tryptophan, phenylalanine	[48]
1291	CH_2 twisting in phospholipids	[37, 38]
1326–1329	CH vibration in DNA/RNA, CH_2 twisting in lipids	[41]
1331	(C–H) Nucleic acid base	[40]
1400	(C–H), Collagen, phospholipids	[41]
1450	$(C\text{-}H_2)$ deformation, Acetoacetate, tryptophan	[37, 38]
1584	(C–C) bending mode of phenylalanine	[40]
1655	(C–O) Amide I, α-helix	[37, 38]

Laser-induced fluorescence is the most common source of interfering baseline signal encountered in Raman measurements. The fluorescence interference in Raman spectroscopy may result from the compound analyzed or from fluorescent impurities in the sample. Autofluorescence background can be produced by tryptophan and tyrosine side chains in folded proteins, by carotenoids and photosynthetic pigments or other chromophores within microbial, animal and plant cells. In addition, it may due to manufacturing additives.

The observed CR and SERS bands are described in Table 1. The major CR peaks are observed at 525, 641, 770, 1100, 1543, 1661 and 1849 cm^{-1} and may be attributed to biochemical components of nucleic acids, fatty acids and Amide I group. For SERS measurements we observe strongly enhanced bands which may be attributed to such biochemical components as nucleic acids (641, 724, 813, 1003, 1210, 1132 and 1450 cm^{-1}), carbohydrates (641, 890, and 1094 cm^{-1}), lipids (1278 and 1327 cm^{-1}), etc. The observed SERS peaks are indicators of the corresponding serum components [29–32].

Several of the observed bands clearly stand out by the impact of SERS technique at 724, 813, 890, 961, and 1132 cm^{-1}. These bands were undetectable by CR spectroscopy, as the intensities of these bands are weaker than the intensity of the autofluorescence and noise signals. The SERS spectrum of serum with AgNPs showed many dominant vibration bands, indicating a strong interaction between the silver colloids and the serum substances. This interaction also indicated that biochemical ingredients in the serum were closely adsorbed onto the surfaces of the AgNPs, and Raman scattering took place in the highly localized optical fields of these structures, which resulted in a strong enhancement in the intensity [29–32].

In SERS spectrum, bands of several molecules could be shifted compared with the bands of these molecules in the CR spectrum. Such shift may be observed from 525, 770, and 1100 cm^{-1} bands to 498, 728, and 1003 cm^{-1} bands respectively. This might be due to the strong interaction between prepared substrate and analyte [33]. It is also found in Fig. 4, which demonstrates the redshift of the SERS spectrum relative to the CR spectrum that observed shift is related to the change of the chemical bond's energy. Some studies have also found the influence of atomic species on the Raman activities. The redshift in SERS is mainly due to the change of the localized plasmons depending on the dielectric functions of metallic nanostructures that, in turn, depend on different parameters, such as the medium, size of NPs, and intrinsic damping of metal, which are known to display this interesting common phenomenon [31]. Moreover, the reason for the blueshift or the redshift of the Raman peak is the change of the corresponding chemical bonds, leading to the migration of electron clouds. Specifically, the change involves the transformation of interatomic bond force and distance [34].

Thus, the spectral bands and SERS characteristics of the serum obtained in the current study are similar to those reported in the studies of other authors. However, Huang et al. and Feng et al. [35, 36] reported SERS bands at 702 cm^{-1} and 1383 cm^{-1} which were not observed in our study; these bands were assigned to the cytosine and CH_3 domains respectively.

The next stage of our research was the analysis of the results repeatability and the stability of the proposed silver substrates. To clarify the central location of the spectral data distribution, a calculation of a mean spectrum was carried out, and the standard deviation of the collected raw spectra was also performed to assess the spread of the values above and below the mean. Such data is presented in Fig. 5 and Fig. 6.

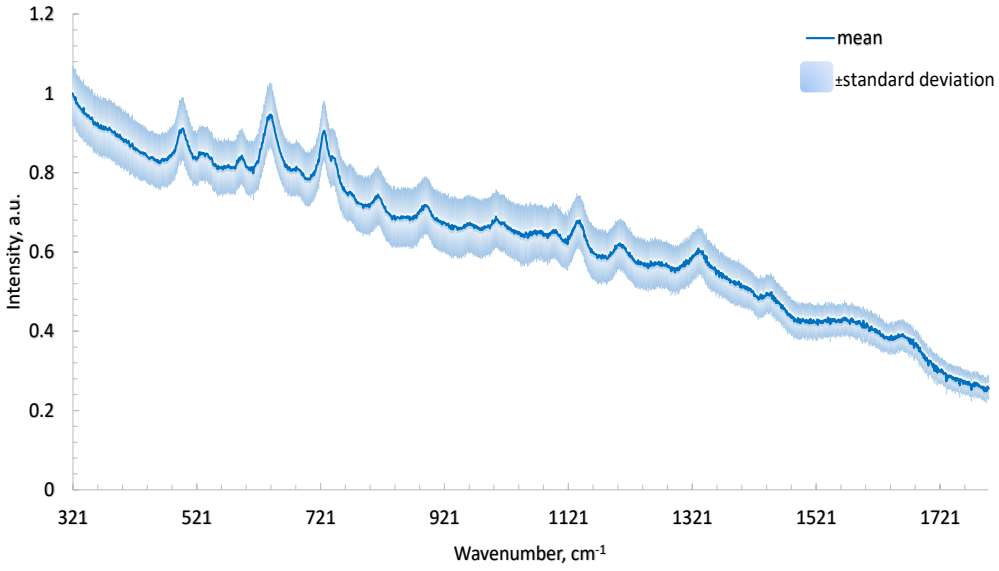

Fig. 5 Mean and standard deviation for human serum sample examined 15 times in the same conditions using single SERS substrate.

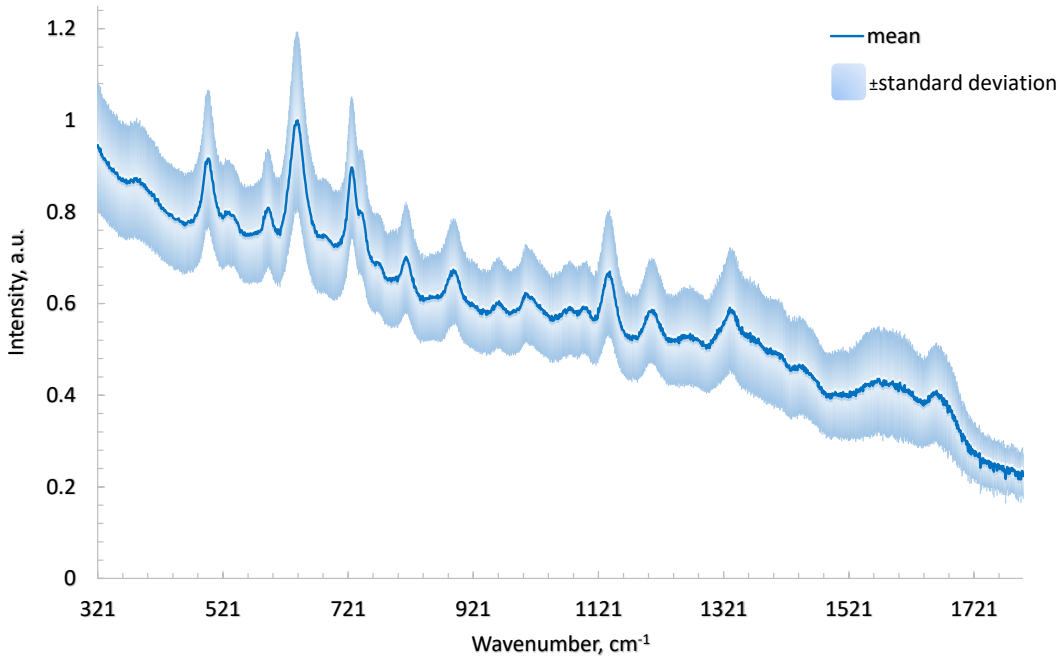

Fig. 6 Mean and standard deviation for serum sample examined for 5 different SERS substrates at 5 different spots.

Table 2 EF values for different spectral bands.

Raman shift (cm^{-1})	I_{Raman}	I_{SERS}	EF
727	0.240	313×10	3.91×10^5
641	131	479×10	1.10×10^3
815	13.4	136×10	3.04×10^3
1132	10.5	231×10	6.60×10^3

The low values of standard deviation show that the data are clustered closely around the mean, thus, the proposed SERS technique is reliable and may be applied in quantitative measurements. In case of a single SERS substrate application maximum standard deviation was up to 8%. In case of different SERS substrates utilization, the standard deviation was up to 19%.

The value of EF depends on the morphology of the NPs. However, the physic-chemical properties of the interfaces, such as the pH, the presence of impurity species, and the available surface on the metal, are also important and may affect the EF value. The interfacial properties of metal surfaces should be considered to understand why certain molecules do not work well in SERS, or why the spectral profile changes from preparation to preparation. The prepared AgNPs were effective and stable, as they are attached to a substrate standing at an appropriate interparticle distance to have a giant electromagnetic enhancement with the formation of hot spots [49]. Lin et al. [50] reported an EF of (5.6×10^9) using gold "pearl necklace" nanomaterials substrate. While Wang et al. [51] found that highly-branched gold nanoparticles provided an EF of (3.6×10^5). However, H. Wang et al. [52] reported an EF of (10^5) for the Ag metalized substrates. The highest EFs observed in the study are collected in Table 2. We found that the largest EF that was calculated from Eq. (1) is detected at 727 cm^{-1} peak and was 3.91×10^5. Note here, that in order to get a higher EFs, it is possible to consider CR bands (I_{Raman}) close to 0, and if newly appeared SERS bands are detected, than the calculated EF value may be extremely high.

The storage stability of the substrates was tested during 1-month period. In this period, we estimated standard deviation of the SERS signal and tracked EF changes. During the tracked period the standard deviation was not higher than the standard deviation observed for single substrate measurements presented above (up to 19%), and EF did not decrease by less than 8%. However, for future possible clinical applications the stability of the substrate should be estimated for a longer period. Important to note, that no blinking phenomenon [53] of SERS spectra from Ag nanoparticles was detected. The term "blinking" is used to describe temporal fluctuations in the Raman spectral signal. It is typically accepted that the observation of blinking behavior in the SERS spectrum is indicative of a single molecule undergoing adsorption/desorption cycles at a SERS "active" site. Blinking in SERS may be attributed to thermal diffusion of a single molecule in and out of hot spots, where

alterations in position of a few nanometers can create a significant change in SERS signal intensity [54, 55]. The intensity of SERS spectra for 5 different SERS substrates at 5 different points and for 15 times in the same condition for one SERS substrate did not change significantly and is within the standard deviation of 19%.

In addition, we showed non-invasiveness of the proposed approach as we examined the serum sample multiple times at the same spot and observed no changes in the intensity for each performed test. It is worth mentioning that the proposed method is quite promising since, unlike previous studies, we employed a non-cooling camera for spectra collection. For instance, Zhou et al. [55] studied SERS effect collecting spectra using a cooling system camera set to –70 °C.

SERS is recognized as an ultrasensitive optical detection technique with wide application potential in a variety of fields due to its great sensitivity at the single molecule level. However, the complex manufacturing and expensive price of SERS substrate remain a barrier to its wide application in industry [56]. Aside from the advantages and limitations of SERS technology in comparison to other diagnostic methods, it is also important to notice that SERS-active substrates are most often fabricated with transition metals (Rh, Pd, Pt, Fe, Co, etc.) and plasmonic metals such as Au and Ag, which have the ability to induce localized surface plasmon resonance, which is a result of the coupling of resonant oscillations of electrons and electromagnetic fields near the nanostructures. However, transition metals have also explored found to impart weaker SERS effects compared to plasmonic metals [57]. In the material selection process, it is also important to consider the suitability of the substrate material in terms of its stability in an environment or condition where it is to be applied. Each plasmonic metal exhibit their own characteristic properties that are not found in other metals; for example, gold is a biocompatible material but provides a lower signal enhancement than silver, which on the other hand is less stable due to it being prone to oxidation [58]. Studies have thus explored the use of both of these metals to take advantage of combining these properties, giving synergistic effects.

Homogeneity is another key point in the evaluation of the SERS substrate, especially when it is used for quantitative detection and imaging. The detection result is reliable only when the results from the substrate are reproducible because SERS is a localized phenomenon and it is highly sensitive to the local structure of the substrate and the surrounding environment. For the NP substrates, the homogeneity in size, shape, and aggregation state will increase the reproducibility. Besides the higher enhancement or better homogeneity, the cost of substrate fabrication should also be considered in SERS applications.

Our proposed approach was found to be considerably easier, faster and more convenient than the methods stated in earlier studies. The colloidal substrates are prepared by either the chemical reduction process or by laser ablation procedures. For instance, Chu et al. [59] proposed a laser ablation-assisted method to fabricate the SERS substrate on the teflon. For the reduction method, Chi et al. [60] created a Silver NP colloidal solution by reducing silver nitrite with sodium citrate in the presence of ultraviolet (UV) light by dropping sodium citrate solution to silver nitrite solution and placing the mixture in a UV chamber. Silicon substrates were immersed in an Ag NP colloidal solution to allow Ag NPs to adhere to the surface. Huang et al. and Zong et al. [35, 61] prepared colloids by adding NaOH solution to hydroxylamine hydrochloride solution and mixing the solution with $AgNO_3$ aqueous solution at room temperature, until the formation of a milky-grey color. The Ag colloids were pelleted by centrifugation. The pelleted Ag NP was then mixed with urine or serum samples at a 1:1 ratio in a rectangle aluminum plate. In another work, Jing et al. [62] used a seed growth technique with AuNPs as seeds to create spherical AgNPs by adding $HAuCl_4$ to deionized water, the solution was heated to boiling. Then, trisodium citrate was immediately added. Serum samples were mixed with the prepared AgNPs solution after cooling. The mixture was transferred to a silicon wafer for SERS analysis.

In comparison to the observed techniques, we have successfully developed a new simple and low-cost AgNPs SERS substrate with excellent sensitivity and promising stability. We obtained excellent SERS spectra using a digital camera without cooling (working at ambient temperature). The proposed technique of blood serum analysis has great potential to significantly increase the application of SERS methods, particularly in clinical applications. Nevertheless, further research in a larger group of collected blood specimens is required to confirm the applicability of the proposed techniques in clinical settings.

4 Conclusion

In this study human blood serum samples were examined using CR and newly proposed SERS technique. To demonstrate the applicability of the proposed technique the serum sample was examined 15 times in the same condition for one SERS substrate and then examined for 5 different SERS substrates at 5 different spots, calculated standard deviation for these cases was up to 8% and up to 19% correspondingly. The obtained results indicate accuracy and stability of the proposed SERS substrates. Demonstrated results shows that the obtained SERS effect helps to achieve up to 4×10^5 EF with silver NPs application for 785 nm laser excitation. Moreover, the proposed SERS technique provides a capability to detect Raman bands 724, 813, 890, 961, and 1132 cm^{-1} which may be attributed to such biochemical components as nucleic acids, carbohydrates, lipids, etc. These bands were not presented in the CR spectra of human serum; thus SERS analysis increases the possibility to detect disease biomarkers during blood samples analysis. The obtained results demonstrate that the proposed SERS technique is stable, no-invasiveness with no blinking phenomenon and has significant potential in clinical diagnosis applications.

Disclosures

All authors declare that there is no conflict of interests in this paper.

Acknowledgments

The study was supported by a grant from the Russian Science Foundation No. 21-75-10097 https://rscf.ru/project/21-75-10097/.

References

1. "Mortality Data", World Health Organization, (accessed 02.02.2022) [https://www.who.int/data/mortality].
2. O. J. Wouters, D. J. O'donoghue, J. Ritchie, P. G. Kanavos, and A. S. Narva, "Early chronic kidney disease: diagnosis, management and models of care," Nature Reviews Nephrology 11(8), 491–502 (2015).
3. S. K. Elwia, S. M. Abo El Wafa, and Y. M. Marei, "The Metabolic Mechanism Underlying the Enhancing Effects of Glycine and Tryptophan on Kidney Function: How to Reduce EGFR Inhibitory Effect on AAs," Egyptian Academic Journal of Biological Sciences, F. Toxicology & Pest Control 13(2), 37–48 (2021).
4. S. Luis-Lima, E. Porrini, "An overview of errors and flaws of estimated GFR versus true GFR in patients with diabetes mellitus," Nephron 136, 287–291 (2017).
5. R. Moynihan, R. Glassock, and J. Doust, "Chronic kidney disease controversy: how expanding definitions are unnecessarily labelling many people as diseased," BMJ 347, f4298 (2013).
6. D.-Q. Chen, G. Cao, H. Chen, D. Liu, W. Su, X.-Y. Yu, N. D. Vaziri, X.-H. Liu, X. Bai, L. Zhang, and Y.-Y. Zhao, "Gene and protein expressions and metabolomics exhibit activated redox signaling and wnt/β-catenin pathway are associated with metabolite dysfunction in patients with chronic kidney disease," Redox biology 12, 505–521 (2017).
7. C. H. Johnson, J. Ivanisevic, and G. Siuzdak, "Metabolomics: beyond biomarkers and towards mechanisms," Nature Reviews Molecular Cell Biology 17(7), 451–459 (2016).
8. P. F. Mulders, "From genes to metabolomics in renal cell carcinoma translational research," European Urology, 2(63), 252–253 (2013).
9. S. Kalim, E. P. Rhee, "An overview of renal metabolomics," Kidney International 91(1), 61–69 (2017).
10. Y. Y. Zhao, "Metabolomics in chronic kidney disease," Clinica Chimica Acta 422, 59–69 (2013).
11. R. H. Weiss, K. Kim, "Metabolomics in the study of kidney diseases," Nature Reviews Nephrology 8(1), 22–33 (2012).
12. L. A. Bratchenko, I. A. Bratchenko, A. A. Lykina, M. V. Komarova, D. N. Artemyev, O. O. Myakinin, A. A. Moryatov, I. L. Davydkin, S. V. Kozlov, and V. P. Zakharov, "Comparative study of multivariative analysis methods of blood Raman spectra classification," Journal of Raman Spectroscopy 51(2), 279–292 (2020).
13. L. A. Bratchenko, I. A. Bratchenko, Y. A. Khristoforova, D. N. Artemyev, D. Y. Konovalova, P. A. Lebedev, and V. P. Zakharov, "Raman spectroscopy of human skin for kidney failure detection," Journal of Biophotonics 14(2), e202000360 (2021).
14. I. A. Bratchenko, L. A. Bratchenko, A. A. Moryatov, Y. A. Khristoforova, D. N. Artemyev, O. O. Myakinin, A. E. Orlov, S. V. Kozlov, and V. P. Zakharov, "In vivo diagnosis of skin cancer with a portable Raman spectroscopic device," Experimental Dermatology 30(5), 652–663 (2021).
15. P. A. Mosier-Boss, "Review of SERS substrates for chemical sensing," Nanomaterials 7(6), 142 (2017).
16. E. Critselis, H. L. Heerspink, "Utility of the CKD273 peptide classifier in predicting chronic kidney disease progression," Nephrology Dialysis Transplantation 31(2), 249–254 (2016).
17. C. Pontillo, L. Jacobs, J. A. Staessen, J. P. Schanstra, P. Rossing, H. J. Heerspink, J. Siwy, W. Mullen, A. Vlahou, H. Mischak, and R. Vanholder, "A urinary proteome-based classifier for the early detection of decline in glomerular filtration," Nephrology Dialysis Transplantation 32(9), 1510–1516 (2017).
18. A. C. Webster, E. V. Nagler, R. L. Morton, and P. Masson, "Chronic kidney disease," The Lancet 389(10075), 1238–1252 (2017).
19. P. Ruggenenti, A. Fassi, A. P. Ilieva, S. Bruno, I. P. Iliev, V. Brusegan, N. Rubis, G. Gherardi, F. Arnoldi, M. Ganeva, and B. Ene-Iordache, "Preventing microalbuminuria in type 2 diabetes," New England Journal of Medicine 351(19), 1941–1951 (2004).
20. E. J. Want, I. D. Wilson, H. Gika, G. Theodoridis, R. S. Plumb, J. Shockcor, E. Holmes, and J. K. Nicholson, "Global metabolic profiling procedures for urine using UPLC–MS," Nature Protocols 5(6), 1005–1018 (2010).
21. A. Bonifacio, S. Dalla Marta, R. Spizzo, S. Cervo, A. Steffan, A. Colombatti, and V. Sergo, "Surface-enhanced Raman spectroscopy of blood plasma and serum using Ag and Au nanoparticles: a systematic study," Analytical and Bioanalytical Chemistry 406(9), 2355–2365 (2014).
22. X. Cao, Z. Wang, L. Bi, and J. Zheng, "Label-free detection of human serum using surface-enhanced raman spectroscopy based on highly branched gold nanoparticle substrates for discrimination of non-small cell lung cancer," Journal of Chemistry 2018, 9012645 (2018).

23. A. Pérez, Y. A. Prada, R. Cabanzo, C. I. González, and E. Mejía-Ospino, "Diagnosis of chagas disease from human blood serum using surface-enhanced Raman scattering (SERS) spectroscopy and chemometric methods," Sensing and Bio-Sensing Research 21, 40–45 (2018).
24. S. Madhuri, N. Vengadesan, P. Aruna, D. Koteeswaran, P. Venkatesan, and S. Ganesan, "Native Fluorescence Spectroscopy of Blood Plasma in the Characterization of Oral Malignancy," Photochemistry and Photobiology 78(2), 197–204 (2003).
25. R. Kalaivani, V. Masilamani, K. Sivaji, M. Elangovan, V. Selvaraj, S. G. Balamurugan, and M. S. Al-Salhi, "Fluorescence spectra of blood components for breast cancer diagnosis," Photomedicine and Laser Surgery 26(3), 251–256 (2008).
26. B. Sharma, R. R. Frontiera, A. I. Henry, E. Ringe, and R. P. Van Duyne, "SERS: Materials, applications, and the future," Materials Today 15(1–2), 16–25 (2012).
27. B. Sardari, M. Özcan, "Real-time and tunable substrate for surface enhanced Raman spectroscopy by synthesis of copper oxide nanoparticles via electrolysis," Scientific Reports 7(1), 7730 (2017).
28. G. M. Herrera, A. C. Padilla, and S. P. Hernandez-Rivera, "Surface enhanced Raman scattering (SERS) studies of gold and silver nanoparticles prepared by laser ablation," Nanomaterials 3(1), 158–172 (2013).
29. A. Subaihi, L. Almanqur, H. Muhamadali, N. AlMasoud, D. I. Ellis, D. K. Trivedi, K. A. Hollywood, Y. Xu, and R. Goodacre, "Rapid, accurate, and quantitative detection of propranolol in multiple human biofluids via surface-enhanced Raman scattering," Analytical Chemistry 88(22), 10884–10892 (2016).
30. E. Witkowska, T. Jagielski, A. Kamińska, A. Kowalska, A. Hryncewicz-Gwóźdź, and J. Waluk, "Detection and identification of human fungal pathogens using surface-enhanced Raman spectroscopy and principal component analysis," Analytical Methods 8(48), 8427–8434 (2016).
31. R. Liu, X. Zi, Y. Kang, M. Si, and Y. Wu, "Surface-enhanced Raman scattering study of human serum on PVA–Ag nanofilm prepared by using electrostatic self-assembly," Journal of Raman Spectroscopy 42(2), 137–144 (2011).
32. J. L. Pichardo-Molina, C. Frausto-Reyes, O. Barbosa-García, R. Huerta-Franco, J. L. González-Trujillo, C. A. Ramírez-Alvarado, G. Gutiérrez-Juárez, and C. Medina-Gutiérrez, "Raman spectroscopy and multivariate analysis of serum samples from breast cancer patients," Lasers in Medical Science 22(4), 229–236 (2007).
33. Q. Liao, M. Y. Li, R. Hao, X. C. Ai, J. P. Zhang, and Y. Wang, "Surface-enhanced Raman scattering and DFT computational studies of a cyanuric chloride derivative," Vibrational Spectroscopy 44(2), 351–356 (2007).
34. H. Ma, S. Liu, N. Zheng, Y. Liu, X. X. Han, C. He, H. Lu, and B. Zhao, "Frequency shifts in surface-enhanced Raman spectroscopy-based immunoassays: mechanistic insights and application in protein carbonylation detection," Analytical Chemistry 91(15), 9376–9381 (2019).
35. Z. Huang, S. Feng, Q. Guan, T. Lin, J. Zhao, C. Y. Nguan, H. Zeng, D. Harriman, H. Li, and C. Du, "Correlation of surface-enhanced Raman spectroscopic fingerprints of kidney transplant recipient urine with kidney function parameters," Scientific Reports 11(1), 2463 (2021).
36. S. Feng, L. Zhou, D. Lin, J. Zhao, Q. Guan, B. Zheng, K. Wang, H. Li, R. Chen, H. Zeng, and C. Du, "Assessment of treatment efficacy using surface-enhanced Raman spectroscopy analysis of urine in rats with kidney transplantation or kidney disease," Clinical and Experimental Nephrology 23(7), 880–889 (2019).
37. N. Stone, C. Kendall, J. Smith, P. Crow, and H. Barr, "Raman spectroscopy for identification of epithelial cancers," Faraday Discussions 126, 141–157 (2004).
38. N. Stone, C. Kendall, N. Shepherd, P. Crow, and H. Barr, "Near-infrared Raman spectroscopy for the classification of epithelial pre-cancers and cancers," Journal of Raman spectroscopy 33(7), 564–573 (2002).
39. J. W. Chan, D. S. Taylor, T. Zwerdling, S. M. Lane, K. Ihara, and T. Huser, "Micro-Raman spectroscopy detects individual neoplastic and normal hematopoietic cells," Biophysical Journal 90(2), 648–656 (2006).
40. S. Feng, R. Chen, J. Lin, J. Pan, Y. Wu, Y. Li, J. Chen, and H. Zeng, "Gastric cancer detection based on blood plasma surface-enhanced Raman spectroscopy excited by polarized laser light," Biosensors and Bioelectronics 26(7), 3167–3174 (2011).
41. J. Lin, R. Chen, S. Feng, J. Pan, Y. Li, G. Chen, M. Cheng, Z. Huang, Y. Yu, and H. Zeng, "A novel blood plasma analysis technique combining membrane electrophoresis with silver nanoparticle-based SERS spectroscopy for potential applications in noninvasive cancer detection," Nanomedicine: Nanotechnology, Biology and Medicine 7(5), 655–663 (2011).
42. J. De Gelder, K. De Gussem, P. Vandenabeele, and L. Moens, "Reference database of Raman spectra of biological molecules," Journal of Raman Spectroscopy: An International Journal for Original Work in all Aspects of Raman Spectroscopy, Including Higher Order Processes, and also Brillouin and Rayleigh Scattering 38(9), 1133–1147 (2007).
43. Z. Movasaghi, S. Rehman, and D. I. ur Rehman, "Fourier transform infrared (FTIR) spectroscopy of biological tissues," Applied Spectroscopy Reviews 43(2), 134–179 (2008).
44. G. Shetty, C. Kendall, N. Shepherd, N. Stone, and H. Barr, "Raman spectroscopy: elucidation of biochemical changes in carcinogenesis of oesophagus," British Journal of Cancer 94(10), 1460–1464 (2006).
45. D. Naumann, "Infrared and NIR Raman spectroscopy in medical microbiology," Proceedings of SPIE 3257, 245–257 (1998).

46. R. J. Lakshmi, V. B. Kartha, C. R. Murali Krishna, J. G. Solomon, G. Ullas, and P. Uma Devi, "Tissue Raman spectroscopy for the study of radiation damage: brain irradiation of mice," Radiation Research 157(2), 175–182 (2002).
47. W. T. Cheng, M. T. Liu, H. N. Liu, and S. Y. Lin, "Micro-Raman spectroscopy used to identify and grade human skin pilomatrixoma," Microscopy Research and Technique 68(2), 75–79 (2005).
48. D. P. Lau, Z. Huang, H. Lui, D. W. Anderson, K. Berean, M. D. Morrison, L. Shen, and H. Zeng, "Raman spectroscopy for optical diagnosis in the larynx: preliminary findings," Lasers in Surgery and Medicine 37(3), 192–200 (2005).
49. M. V. Canamares, J. V. Garcia-Ramos, S. Sanchez-Cortes, M. Castillejo, and M. Oujja, "Comparative SERS effectiveness of silver nanoparticles prepared by different methods: A study of the enhancement factor and the interfacial properties," Journal of Colloid and Interface Science 326(1), 103–109.
50. Z. H. Lin, I. C. Chen, and H. T. Chang, "Detection of human serum albumin through surface-enhanced Raman scattering using gold "pearl necklace" nanomaterials as substrates," Chemical Communications 47(25), 7116–7118 (2011).
51. Z. Y. Wang, W. Li, Z. Gong, P. R. Sun, T. Zhou, and X. W. Cao, "Detection of IL-8 in human serum using surface-enhanced Raman scattering coupled with highly-branched gold nanoparticles and gold nanocages," New Journal of Chemistry 43(4), 1733–1742 (2019).
52. H. Wang, N. Malvadkar, S. Koytek, J. Bylander, W. B. Reeves, and M. C. Demirel, "Quantitative analysis of creatinine in urine by metalized nanostructured parylene," Journal of Biomedical Optics 15(2), 027004 (2010).
53. C. Popa, M. Petrus, and A. M. Bratu, "Ammonia and ethylene biomarkers in the respiration of the people with schizophrenia using photoacoustic spectroscopy," Journal of Biomedical Optics 20(5), 057006 (2015).
54. Y. Kitahama, "Observation and analysis of blinking surface-enhanced Raman scattering," Journal of Visualized Experiments 131, e56729 (2018).
55. Y. Zhu, C. S. Choe, S. Ahlberg, M. C. Meinke, A. Ulrike, J. M. Lademann, and M. E. Darvin, "Penetration of silver nanoparticles into porcine skin ex vivo using fluorescence lifetime imaging microscopy, Raman microscopy, and surface-enhanced Raman scattering microscopy," Journal of Biomedical Optics, 20(5), 051006 (2014).
56. Y. S. Huh, A. J. Chung, and D. Erickson, "Surface enhanced Raman spectroscopy and its application to molecular and cellular analysis," Microfluidics and Nanofluidics 6(3), 285–297 (2009).
57. M. Sharifi, S. H. Hosseinali, R. H. Alizadeh, A. Hasan, F. Attar, A. Salihi, M. S. Shekha, K. M. Amen, F. M. Aziz, A. A. Saboury, and K. Akhtari, "Plasmonic and chiroplasmonic nanobiosensors based on gold nanoparticles," Talanta 212, 120782 (2020).
58. Y. L. Liu, J. Zhu, G. J. Weng, J. J. Li, and J. W. Zhao, "Gold nanotubes: synthesis, properties and biomedical applications," Microchimica Acta 187(11), 612 (2020).
59. F. Chu, S. Yan, J. Zheng, L. Zhang, H. Zhang, K. Yu, X. Sun, A. Liu, and Y. Huang, "A simple laser ablation-assisted method for fabrication of superhydrophobic SERS substrate on Teflon film," Nanoscale Research Letters 13(1), 244 (2018).
60. J. Chi, T. Zaw, I. Cardona, M. Hosnain, N. Garg, H. R. Lefkowitz, P. Tolias, and H. Du, "Use of surface-enhanced Raman scattering as a prognostic indicator of acute kidney transplant rejection," Biomedical Optics Express 6(3), 761–769 (2015).
61. M. Zong, L. Zhou, Q. Guan, D. Lin, J. Zhao, H. Qi, D. Harriman, L. Fan, H. Zeng, and C. Du, "Comparison of Surface-Enhanced Raman Scattering Properties of Serum and Urine for the Detection of Chronic Kidney Disease in Patients," Applied Spectroscopy 75(4), 412–421 (2021).
62. J. Guo, Z. Rong, Y. Li, S. Wang, W. Zhang, and R. Xiao, "Diagnosis of chronic kidney diseases based on surface-enhanced Raman spectroscopy and multivariate analysis," Laser Physics 28(7), 075603 (2018).